Journal of University of Science and Technology Beijing
Volume 11, Number 3, June 2004, Page 273

Numerical simulation of strain localization and damage evolution in large plastic deformation using mixed finite element method

Zhanghua Chen, Jiajian Jin, and Jiumei Xiao

Applied Science School, University of Science and Technology Beijing, Beijing 100083, China
(Received 2003-05-27)

Abstract: An investigation of computer simulation is presented to analyze the effects of strain localization and damage evolution in large plastic deformation. The simulation is carried out by using an elastic-plastic-damage coupling finite element program that is developed based on the concept of mixed interpolation of displacement/pressure. This program has been incorporated into a damage mechanics model as well as the corresponding damage criterion. To illustrate the performance of the proposed approach, a typical strain localization problem has been simulated. The results show that the proposed approach is of good capability to capture strain localization and predict the damage evolution.

Key words: strain localization; mixed element; Truesdell stress rate; material damage

[*The work was financially supported by a research grant from University of Science and Technology Beijing (No.20020611590).*]

1 Introduction

In engineering application, prediction of failure due to material damage is curial important because the occurrence of macroscopic fracture in metal forming process is frequently induced by the gradual growth of material micro-defects known as internal damage. Therefore, the effect of internal damage resulting from the strain localization should not be neglected. Up to now, both theoretical analysis and numerical simulation have been widely applied to describe this phenomenon.

The finite-element method has long been used as a means of reliable computation to analyze various metal forming processes. Using the finite element method, a complete process of complex deformation can be simulated. In order to take material imperfections into consideration, Doege [1] and Brunet [2] have applied Gurson's model to simulate the deep-drawing process and compute the forming limit diagram for sheet metal forming process. When Gurson's model is applied to simulate the strain localization phenomenon including diffused necking and localized necking, one should pay attention to some problems existing in this model. Since Gurson's model is originally developed for porous materials, it is especially suitable for simulating spherical voids grow during the deformation process. However, porous materials are rarely used in metal forming application. In addition, it is difficult to measure the magnitude of void growth in a forming process.

Under large plastic deformation, the nucleation, growth and coalescence of micro-defects take place due to high stress triaxiality and it is usually referred to as strain damage [3,4]. In this study, a computational model based on the continuum damage mechanics (CDM) instead of Gurson's model has been employed to predict the damage evolution and cracking. A damage variable [5] is incorporated into the consistent elasto-plastic constitutive equation. A typical necking problem of the cylindrical bar under the tension is chosen to validate the proposed model. Using the mixed u/p finite element program together with a damage-based criterion, the numerical simulation is therefore performed. Damage distribution is also discussed.

2 Mixed finite element formulation

In a typical time interval $[t_n, t_{n+1}]$, the variational formulation of the classical weak form of momentum balance in a spatial description restricted to the static case leads to

$$\int_{\Omega_{n+1}} \boldsymbol{\sigma}_{n+1} : \delta \boldsymbol{d} \mathrm{d}v = G_{n+1}^{\mathrm{ext}}(\delta \boldsymbol{d}) \quad (1)$$

where Ω_{n+1} denotes the current configuration at time

Corresponding author: Zhanghua Chen, **E-mail:** czhhylchj@sina.com

t_{n+1}, σ_{n+1} is the Cauchy stress, $d = \frac{1}{2}\left[\nabla v + (\nabla v)^{\mathrm{T}}\right]$ denotes the tensor of the deformation rate, G^{ext} is the virtual work of the external loading. This equation can be treated as a variational principle equation for the determination of the stationary point of a functional Π_{n+1} in which the incremental displacement field $\Delta u(t) = x_{n+1} - x_n$ is taken as the only variable in the boundary-value problem. For the high degree of non-linearity, equation (1) needs to be linearized and solved by iteration. By adopting incremental finite element approach, an efficient and stable iterative technique is employed to solve the discretized equilibrium equations for each time step. The linearization of equation (1) can be formulated in terms of the Truesdell stress rate and the virtual displacement δu:

$$\int_{\Omega_{n+1}}\left[\mathrm{d}\sigma^{\mathrm{TR}} + \sigma : (\nabla \mathrm{d}u)\cdot(\nabla \delta u)^{\mathrm{T}}\right]\mathrm{d}v = \mathrm{d}G_{n+1}^{\mathrm{ext}}(\delta u) \quad (2)$$

where $\mathrm{d}\sigma^{\mathrm{TR}}$ is the Truesdell rate of Cauchy stress. The Truesdell rate is related to the rotation neutralized stress σ^{NR} by the following expression [6]:

$$\sigma^{\mathrm{NR}} = R^{\mathrm{T}}\cdot\sigma_n\cdot R + C^{\mathrm{EP}} : \int_{t_n}^{t_{n+1}} d^{\mathrm{NR}}\mathrm{d}\tau \quad (3)$$

$$\mathrm{d}\sigma^{\mathrm{TR}} = R\cdot\mathrm{d}\sigma^{\mathrm{NR}}\cdot R^{\mathrm{T}} - \sigma\cdot\mathrm{d}\varepsilon - \mathrm{d}\varepsilon\cdot\sigma \quad (4)$$

where R denotes the rotation tensor.

Starting from the decomposition of the Cauchy stress tensor into its deviatoric component s and hydrostatic pressure p, *i.e.*

$$\sigma = s - p1 \quad (5)$$

where $s = \mathrm{dev}(\sigma)$, $p = -\frac{1}{3}\mathrm{tr}(\sigma)$. For the rate-independent metal material, a constrained condition should be supplemented as

$$\mathrm{div}(u) + \frac{p}{K} = 0 \quad (6)$$

where $\mathrm{div}(\bullet)$ denotes the divergence operator, and K denotes the bulk modulus.

The variational formulation should be recast by taking s and p as independent variables:

$$\int_{\Omega_{n+1}}\left[s : \mathrm{dev}(\nabla\delta u) - p\cdot\mathrm{div}(\delta u)\right]\mathrm{d}v = G_{n+1}^{\mathrm{ext}}(\delta u) \quad (7)$$

$$\int_{\Omega_{n+1}}\left[-\delta p\cdot\left(\frac{p}{K} + \mathrm{div}(u)\right)\right]\mathrm{d}v = 0 \quad (8)$$

Furthermore, the discrete mixed u/p finite element equations can be deduced by the linearization of the above variational formulations. In the case of constant pressure within a 4-node bilinear element, the equation can be simplified as

$$\left[K^{\mathrm{EP}}\right]\{\Delta u\} = \left(\left[K^{\mathrm{G}}\right] + \left[K_{\mathrm{v}}^{\mathrm{EP}}\right] + \left[K_{\mathrm{d}}^{\mathrm{EP}}\right]\right)\{\Delta u\} = \{\Delta\Psi\} \quad (9)$$

where

$$K^{\mathrm{G}} = \int_{\Omega} G^{\mathrm{T}}\cdot\sigma_n\cdot G\mathrm{d}v \quad (10)$$

$$K_{\mathrm{v}}^{\mathrm{EP}} = \int_{\Omega} K\bar{B}_{\mathrm{v}}^{\mathrm{T}}\cdot\bar{B}_{\mathrm{v}}\mathrm{d}v \quad (11)$$

$$K_d^{\mathrm{EP}} = \int_{\Omega} B^{\mathrm{T}}\cdot\left(\bar{C}^{\mathrm{EP}} - \Lambda\right)\cdot B\mathrm{d}v \quad (12)$$

and

$$\bar{B}_v = \frac{\int_{\Omega} B_{\mathrm{v}}\mathrm{d}v}{\int_{\Omega}\mathrm{d}v} \quad (13)$$

$$\left(\bar{C}^{\mathrm{EP}}\right)_{ijkl} = \bar{p}\cdot(\delta_{ij}\cdot\delta_{kl}) + R_{iI}\cdot R_{jJ}\cdot R_{kK}\cdot R_{lL}\cdot C_{IJKL}^{\mathrm{EP}} \quad (14)$$

$$C^{\mathrm{EP}} = K1\otimes 1 + 2G\beta\left[I - \tfrac{1}{3}1\otimes 1\right] - 2\mu\gamma N_{n+1}\otimes N_{n+1} \quad (15)$$

$$\begin{cases} \beta = \dfrac{\sigma_{n+1}}{\sigma_{n+1}^{\mathrm{trial}}} \\ \gamma = \dfrac{3\mu}{3\mu + h} - (1-\beta) \\ N_{n+1} = \dfrac{\sigma_{n+1}^{\mathrm{trial}}}{\left\|\sigma_{n+1}^{\mathrm{trial}}\right\|} \end{cases} \quad (16)$$

$$(\Lambda)_{ijkl} = \tfrac{1}{2}\left(\sigma_{ik}\cdot\delta_{lj} + \sigma_{jl}\cdot\delta_{ki} + \sigma_{jk}\cdot\delta_{li} + \sigma_{il}\cdot\delta_{kj}\right) \quad (17)$$

$$\sigma_{n+1} = \left(\mathrm{dev}(\sigma_{n+1}) - \bar{p}_{n+1}\cdot 1\right) \quad (18)$$

$$\Delta\Psi = F^{\mathrm{ext}} - \int_{\Omega} B^{\mathrm{T}}\cdot\sigma_{n+1}\mathrm{d}v \quad (19)$$

where 1 is a second order identity tensor and I is the fourth order identity tensor. K^{G} is the standard geometrical stiffness matrix, B_{v} denotes the dilatation part of the strain interpolation matrix B, μ denotes the shear modulus, and $\bar{C}^{\mathrm{EP}}$ denotes the equivalent consistent elasto-plastic module which is rewritten following the original concept proposed by Simo [7]. It is well known that if the incompatible element method is employed to tackle the incompressible problem, the Babuška-Brezzi condition must be satisfied [8]. For using a 4-node bilinear element with constant pressure, a post-processing procedure proposed by Hughes [9] can satisfied this requirement.

3 Integration of the constitutive equations

Up to now some well-known objective stress rates such as the Jaumann rate and the Green-Naghdi rate have been implemented in commercial codes, however, they exhibit the path dependence. Therefore, the Truesdell rate may be an appropriated choice for isotropic hardening materials as discussed in reference [10]. Moreover, the corotational approach [6] provides a rotation neutralized strain measure and it is independent from the rotation tensor $\boldsymbol{R}$. In this approach, the rotation neutralized deformation rate tensor can be written as

$$\boldsymbol{d}^{\mathrm{NR}} = \boldsymbol{R}^{\mathrm{T}} \cdot \boldsymbol{d} \cdot \boldsymbol{R} = \tfrac{1}{2}\left(\dot{\boldsymbol{U}}\boldsymbol{U}^{-1} + \boldsymbol{U}^{-1}\dot{\boldsymbol{U}}\right) \tag{20}$$

In this equation, if the $\boldsymbol{R}$ is associated with the deformation of the material body between the reference configuration Ω_n and the current configuration Ω_{n+1}, it can be evaluated from the polar decomposition of the incremental deformation gradient $\boldsymbol{F}_{\mathrm{inc}}$:

$$\begin{cases} \boldsymbol{F}_{\mathrm{inc}} = \dfrac{\partial \boldsymbol{x}_{n+1}}{\partial \boldsymbol{x}_n} \\ \boldsymbol{F}_{\mathrm{inc}} = \boldsymbol{R}_{n+1} \cdot \boldsymbol{U}_{n+1} \\ J = \det(\boldsymbol{F}_{\mathrm{inc}}) > 0 \end{cases} \tag{21}$$

where $\boldsymbol{U}$ is the corresponding right stretch tensor. According to the material description of motion, the rate form of the constitutive equation can be written as

$$\dot{\boldsymbol{\sigma}}^{\mathrm{NR}} = \boldsymbol{C}^{\mathrm{EP}} : \boldsymbol{d}^{\mathrm{NR}} \tag{22}$$

where the superscript 'NR' denotes the neutralization of rotation. According to the material description of motion, the integration of the constitutive equation by means of rotation-neutralized transformation can be expressed as

$$\begin{aligned} \boldsymbol{\sigma}_{n+\frac{1}{2}} &= \boldsymbol{R}_{n+\frac{1}{2}} \cdot \left(\boldsymbol{R}^{\mathrm{T}}_{n+\frac{1}{2}} \cdot \boldsymbol{\sigma}_n \cdot \boldsymbol{R}_{n+\frac{1}{2}} + \Delta\boldsymbol{\sigma} \right) \cdot \boldsymbol{R}^{\mathrm{T}}_{n-\frac{1}{2}} \\ &= \boldsymbol{R}_{n+\frac{1}{2}} \cdot \left(\boldsymbol{R}^{\mathrm{T}}_{n+\frac{1}{2}} \cdot \boldsymbol{\sigma}_n \cdot \boldsymbol{R}_{n+\frac{1}{2}} + \boldsymbol{C}^{\mathrm{ep}} : \int_{t_n}^{t_{n+1}} \boldsymbol{d}^{\mathrm{NR}} \mathrm{d}\tau \right) \cdot \boldsymbol{R}^{\mathrm{T}}_{n+\frac{1}{2}} \end{aligned} \tag{23}$$

where $\boldsymbol{R}$ denotes the incremental rotation tensor which is obtained from the polar decomposition of the deformation gradient, the subscript $n+\frac{1}{2}$ means that rotation operation performed at the position of mid-interval between the reference configuration $\boldsymbol{x}_n$ and the current configuration $\boldsymbol{x}_{n+1}$, and the superscript 'NR' denotes neutralized rotation. The velocity $\boldsymbol{v}$ of material particles is considered to be constant and $\boldsymbol{d}$ is also kept constant at the mid-interval. Therefore, the integration of constitutive equation within the time interval $[t_n, t_{n+1}]$ can be simplified as

$$\begin{aligned} \int_{t_n}^{t_{n+1}} \boldsymbol{d}^{\mathrm{NR}} \mathrm{d}\tau &= \Delta\boldsymbol{\varepsilon}^{\mathrm{NR}} \\ &\approx \boldsymbol{R}^{\mathrm{T}}_{n+\frac{1}{2}} \cdot \left[\left(\nabla_{x+\frac{1}{2}} \Delta\boldsymbol{u}\right) + \left(\nabla_{x+\frac{1}{2}} \Delta\boldsymbol{u}\right)^{\mathrm{T}} \right] \cdot \boldsymbol{R}_{n+\frac{1}{2}} \\ &= \boldsymbol{R}^{\mathrm{T}}_{n+\frac{1}{2}} \cdot \Delta\boldsymbol{\varepsilon} \cdot \boldsymbol{R}_{n+\frac{1}{2}} \end{aligned} \tag{24}$$

where $\nabla_{x+\frac{1}{2}}$ is the gradient operator taken in the mid-increment position, and $\Delta\boldsymbol{u} = \boldsymbol{u}_{n+1} - \boldsymbol{u}_n$ is the incremental displacement at the time t_{n+1}. By applying the split of the Cauchy stress $\boldsymbol{\sigma}_{n+1} = \mathrm{dev}(\boldsymbol{\sigma}_{n+1}) - p_{n+1}\boldsymbol{I}$ into equation (23), the corresponding formulations can be written as

$$\begin{aligned} p_{n+1} &= \boldsymbol{R}_{n+\frac{1}{2}} \cdot \left(p_n \boldsymbol{I} + K(\boldsymbol{I} \otimes \boldsymbol{I}) : \int_{t_n}^{t_{n+1}} \boldsymbol{R}^{\mathrm{T}}_{n+\frac{1}{2}} \cdot \boldsymbol{d} \cdot \boldsymbol{R}_{n+\frac{1}{2}} \mathrm{d}\tau \right) \cdot \boldsymbol{R}^{\mathrm{T}}_{n+\frac{1}{2}} \\ &= (p_n + K\ln J)\boldsymbol{I} \end{aligned} \tag{25}$$

$$\begin{aligned} &\mathrm{dev}(\boldsymbol{\sigma}_{n+1}) \\ &= \boldsymbol{R}_{n+\frac{1}{2}} \cdot \left(\mathrm{dev}(\boldsymbol{\sigma}_{n+1}) + \boldsymbol{C}^{\mathrm{dev}}_{\mathrm{ep}} : \int_{t_n}^{t_{n+1}} \boldsymbol{R}^{\mathrm{T}}_{n+\frac{1}{2}} \cdot \boldsymbol{d} \cdot \boldsymbol{R}_{n+\frac{1}{2}} \mathrm{d}\tau \right) \cdot \boldsymbol{R}^{\mathrm{T}}_{n+\frac{1}{2}} \end{aligned} \tag{26}$$

In deriving the above equations, the relation $\boldsymbol{I} : \boldsymbol{d} \equiv d_{kk} = \dot{J}/J$ is introduced.

For integrating the isotropic material response given in the rate form (26), the well-known radial return algorithm of the finite deformation [11] has been used.

4 Damage model

For elastic deformation, the hypothesis of strain equivalence proposed by Lemaitre is adopted. Hence, the relationship between the effective and the true elastic module is expressed as $\tilde{E} = (1-D)E$ and $\tilde{\nu} = \nu$. The stress-strain relation is

$$\tilde{s} = 2Ge^{\mathrm{e}} \tag{27}$$

$$\tilde{\sigma}_{\mathrm{kk}} = 3K\sigma^{\mathrm{e}}_{\mathrm{kk}} \tag{28}$$

where s and e are the tensors of the deviatoric stress and strain, respectively. G and K are the shear modulus and the bulk modulus, respectively. For plastic deformation, isotropic hardening is assumed and it is expressed in terms of an internal variable, *i.e.* the equivalent plastic strain. The classical hypothesis of generalized standard materials and the associated plasticity are adopted. With the use of the consistency condition and normality law, the constitutive plastic equations incorporating material damage may be derived as

$$\Delta e^{\mathrm{p}} = \frac{3}{2}\frac{\tilde{s}}{\sigma_{\mathrm{eq}}}\Delta\bar{\varepsilon}_{\mathrm{p}} \tag{29}$$

By substituting equation (29) into (27), it can be obtained that

$$\tilde{s} = 2G\left(e^{\mathrm{e}}|_t + \Delta e - \frac{3}{2}\frac{\tilde{s}}{\sigma_{\mathrm{eq}}}\Delta\bar{\varepsilon}_{\mathrm{p}}\right) \tag{30}$$

For simplicity of notation, it is written $\hat{e} = e^{\mathrm{e}}|_t + \Delta e$. Hence the above equation becomes

$$\left(1 + \frac{3G\Delta\bar{\varepsilon}_{\mathrm{p}}}{\sigma_{\mathrm{eq}}}\right)\tilde{s} = 2G\hat{e} \tag{31}$$

The inner product of this equation with itself gives

$$\sigma_{eq} + 3G\Delta\bar{\varepsilon}_p = 3G(1-D)\tilde{e} \tag{32}$$

where $\tilde{e} = \sqrt{2/3\, e_{ij} \cdot e_{ij}}$. The tangent elasto-plastic-damage coupling stiffness matrix can be set up by taking the effect of the damage into equations (11) and (12). In this case, the modulus in equations (11), (15) and (16) should be replaced in terms of the effective modulus, *i.e.*,

$$\tilde{K} = K(1-D), \quad \tilde{h} = h(1-D) \tag{33}$$

It is obvious that the elasto-plastic-damage coupling stiffness matrix is still a symmetric matrix.

5 Damage evolution

For the isotropic materials, it is reasonable to use Lemaitre's damage evolution that is valid for most engineering applications [2-5]. The incremental relation between damage and stress is given as

$$\dot{D} = \left(\frac{Y}{S}\right)^q \frac{d\bar{\varepsilon}_p}{dt} H(\bar{\varepsilon}_p - \bar{\varepsilon}_p|_D) \tag{34}$$

In the above equation, q is the material dependent parameter, $\bar{\varepsilon}_p|_D$ denotes the strain threshold for micro-cracking. H is a step function and Y is defined as

$$Y = -\partial W^e / \partial D = -\frac{1}{2}\boldsymbol{\varepsilon}^T : E : \boldsymbol{\varepsilon} \tag{35}$$

where W^e is the elastic strain energy density. For linear isotropic elasticity, Y is the damage strain energy release rate. This quantity may be used as a damage criterion by the definition from a one-dimensional equivalent stress [5]. The damage evolution equation is obtained by substituting equations (35) into (34)

$$\dot{D} = \left(\frac{\sigma_{eq} R_v}{2ES(1-D)^2}\right)^q \frac{d\bar{\varepsilon}_p}{dt} H(\bar{\varepsilon}_p - \bar{\varepsilon}_p|_D) \tag{36}$$

where R_v denotes the stress triaxiality. In order to perform the finite element analysis, the incremental form of the above equation is required. By applying the backward Euler method for the state at the end of the increment, the damage increment can be expressed as

$$\Delta D = \left(\frac{\sigma_{eq} R_v}{2ES(1-D)^2}\right)^q \Delta\bar{\varepsilon}_p H(\bar{\varepsilon}_p - \bar{\varepsilon}_p|_D) \tag{37}$$

Next, the attention is devoted to determine the incremental equivalent plastic strain $\Delta\bar{\varepsilon}_p$. The von Mises equivalent stress must satisfy the uniaxial form, so that from equation (32).

$$3G\left[(1-D)\tilde{e} - \Delta\bar{\varepsilon}_p\right] = \sigma_{eq} = (1-D)\{R_0 + R(\bar{\varepsilon}_p)\} \tag{38}$$

This nonlinear equation can be solved by the local Newton's method:

$$\Delta\bar{\varepsilon}_p|_{k+1} = \Delta\bar{\varepsilon}_p|_k + c_k, \quad \Delta\bar{\varepsilon}_p|_0 = 0 \tag{39}$$

accompanying with

$$c_k = \frac{(1-D)\{R_0 + R(\bar{\varepsilon}_p)\} - 3G\left[(1-D)\tilde{e} - \Delta\bar{\varepsilon}_p|_k\right]}{3G + (1-D)H_k} \tag{40}$$

Once $\Delta\bar{\varepsilon}_p$ is known, the damage increment ΔD and the damage variable D can be determined in terms of equation (37). This method is suitable for non-proportional loading as well as proportional one. It is assumed that ductile failure would occur if the damage D reaches its critical value D_{cr}, *i.e.*,

$$D = D_{cr} \tag{41}$$

In this study, $D_{cr} = 0.46$ is obtained from the standard tensile tests. This value is taken as the critical damage parameter and it may be considered as a material property.

6 Numerical examples

To validate the mixed FEM, a representative example proposed by Simo [7] was selected. The example is the necking of a cylindrical bar under the finite stretching. Due to the symmetry, only quarter of the bar is modeled with 6.413 mm in width and 26.667 mm in length. To trigger necking, a width reduction of 1.8% is introduced in the center of the bar. The finite element mesh consists of 2×12×12 elements. The material is assumed to obey the general saturation isotropic hardening constitutive equation:

$$\sigma_y = \sigma_0 + (\sigma_\infty - \sigma_0)[1 - \exp(-\delta \cdot \bar{\varepsilon}_p)] + H \cdot \bar{\varepsilon}_p \tag{42}$$

The values of material parameters used in the computation are the same as those published in reference [7], *i.e.*, E = 206.9 GPa, ν = 0.29, σ_0 = 0.45 GPa, σ_∞ = 0.715 GPa, δ = 16.93, H = 0.12924 GPa. Totally 50 uniform time steps were applied to simulate a prescribed vertical displacement u = 7.0 mm on the top edge of the mesh. The simulation result is illustrated in **figure 1**. The load-displacement curve of the problem solved by using the proposed element has been compared with Simo's work as shown in **figure 2**. The present approach has good performance to capture strain localization in spite of its slight more rigid stiffness. It should be noticed that no spurious hourglassing in the localized region has been observed even the tremendously deformation.

With the consideration of damage, necking takes place in the mid-plane of the bar. This localization phenomenon occurs due to micro-void and micro-crack nucleation, growth and coalescence that reduce the effective area of load bearing. Consequently, the deterioration of material properties inevitably happens, this may be referred to as damage softening. The damage distribution under given displacement is illustrated in **figure 3**. It is observed that the damage concentrates near the mid-plane of the bar. There is almost no damage occurring outside this region. Damage develops rapidly during the later part of the loading history. Finally, damage reaches its critical value at the center of the bar where the material rupture occurs.

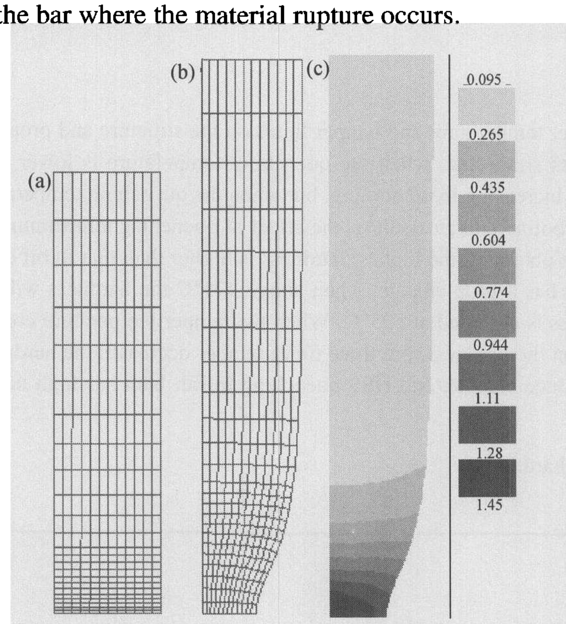

Figure 1 Axisymmetric necking: (a) initial geometry and finite element mesh; (b) final deformed mesh (u=7.0); (c) distribution of equivalent plastic strain.

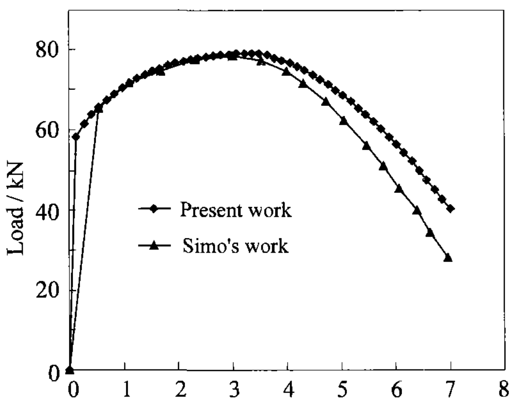

Figure 2 Load-displacement curves for the axisymmetric necking problem.

7 Conclusions

A mixed u/p finite element method based on Truesdell stress rate has been developed successfully for simulating large plastic deformation problems including strain localization and material damage. Numerical results show that this approach is of good ability to capture strain localization and predict the damage evolution. This approach is suitable for simulation of metal forming problems especial when the effect of damage cannot be neglected.

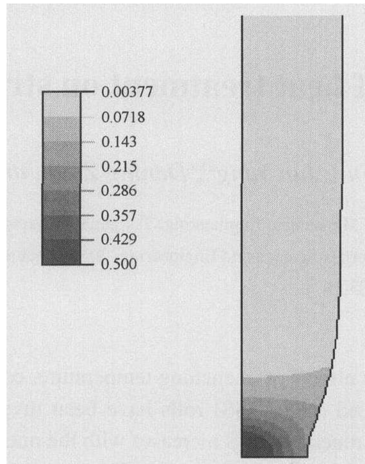

Figure 3 Damage distribution in deformed bar.

References

[1] E. Doege, T. El-Dsoki, and D. Seibert, Prediction of necking and wrinkling in sheet-metal forming [J], *J. Mater Proc. Technol.*, 50(1995), p.197.

[2] M. Brunet, S. Mguil, and F. Morestin, Analytical and experimental studies of necking in sheet metal forming processes [J], *J. Mater Proc. Technol.*, 80-81(1998), p.40.

[3] C.Y. Tang, W. Shen, and T. C. Lee, A damage-based criterion for fracture prediction in metal forming processes: A case study in Al 2024T3 sheet [J], *J. Mater Proc. Technol.*, 89-90(1999), p.79.

[4] C.Y. Tang, W. Shen, L.C. Fung, et al, Second-order continuity tensor and stiffness degradation of aluminum alloy 2024T3 under large strain at room temperature [J], *Int. J. Mech. Sci.*, 42(2000), p.87.

[5] J. Lemaitre and J.P. Sermerg, One damage law for different mechanisms [J], *Comput. Mech.*, 20(1997), p.84.

[6] J.C. Nagtegaal and N. Rebelo, On the development of a general purpose finite element program for analysis of forming process [J], *Int. J. Numer. Methods Eng.*, 25 (1988), p.113.

[7] J.C. Simo and R.L. Taylor, Consistent tangent operators for rate-independent elastoplasticity [J], *Comput. Methods Appl. Mech. Eng.*, 48(1985), p.101.

[8] T.J.R. Hughes, L.P. Franca, and M. Balestra, A new finite element formulation for fluid dynamics, V. Circumventing the Babuška-Brezzi condition: a stable Petrov-Galerkin formulation of the Stokes problem accommodating equal order interpolation [J], *Comput. Methods Appl. Mech. Eng.*, 59(1986), p.85.

[9] T.J.R. Hughes, *The Finite Element Method — Linear Static and Dynamic Finite Element Analysis* [M], Prentice-Hall, Inc., 1987.

[10] A.F. Marcon, E. Bittencourt, and G.J. Creus, On the integration of stresses in large deformations plasticity [J], *Eng. Comput.*, 16(1999), p.49.

[11] T.J.R. Hughes, *Theoretical Foundation for Large-Scale Computations for Nonlinear Material Behavior* [M], Martinus Nijhoff Publishers, Dordrecht, 1984.